Bioelectrochemistry 148 (2022) 108273

Contents lists available at ScienceDirect

Bioelectrochemistry

journal homepage: www.journals.elsevier.com/bioelectrochemistry

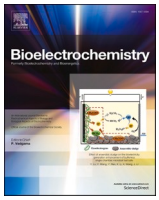

Application of egg yolk IgY on carboxylated polypyrrole films for impedimetric detection of *Pf*HRP2 antigen

Ariamna María Dip Gandarilla [a,*], Juliane Correa Glória [b], Yonny Romaguera Barcelay [c], Rodrigo F.B. de Souza [d], Luís André Morais Mariuba [b], Walter Ricardo Brito [a,*]

[a] *Department of Chemistry, Federal University of Amazonas, Manaus, Amazonas 69067-005, Brazil*
[b] *Leônidas and Maria Deane Institute, Oswaldo Cruz Foundation, Manaus, Amazonas 69057-070, Brazil*
[c] *Physics Department, Federal University of Amazonas, Manaus, Amazonas, 69067-005. Brazil*
[d] *Instituto de Pesquisas Energéticas e Nucleares - IPEN/CENEN, São Paulo 05508-000, Brazil*

ARTICLE INFO

Keywords:
IgY antibodies
Polypyrrole films
Histidine-rich protein 2
Impedimetric immunosensor
Screen-printed gold electrodes
Malaria

ABSTRACT

This paper described an impedimetric immunosensor for detecting *Plasmodium falciparum* histidine-rich protein 2 (*Pf*HRP2). Antibodies from egg yolk (Ab-*Pf*HRP2, IgY type) were linked covalently to the screen-printed gold electrodes (SPGE) surface modified with a thin film of Poly-pyrrole-pyrrole 3 carboxylic acid (P(Py-Py3COOH) to develop the sensing platform. The fabrication steps were followed by microscopic (scanning electron microscopy), spectroscopic (RAMAN spectroscopy and Energy-dispersive X-ray spectroscopy), and electrochemical (electrochemical impedance spectroscopy (EIS) and cyclic voltammetry) techniques. The determination of Ag-*Pf*HRP2 was performed by EIS, and the BSA(bovine serum albumin)/Ab-*Pf*HRP2(IgY)/P(Py-Py3COOH)/SPGE immunosensor recorded a linear response at 100–1000 ng mL^{-1} concentration range, with a limit of detection (LOD) of 27.47 ng mL^{-1}. Its performance was confirmed by Enzyme-Linked Immuno-Sorbent Assay. The fabricated device uses a simple strategy of IgY immobilization, showing high sensitivity and good selectivity, and can be considered an alternative for carrying out malaria tests.

1. Introduction

Malaria is an infectious disease caused by *Plasmodium* sp. protozoa and transmitted to humans by the *Anopheles* female mosquito. Globally, malaria is distributed in six regions, affecting fundamentally tropical and subtropical countries. The World Health Organization estimated 229 million cases in 2019 and reported 409,000 deaths [1,2]. In South America, Brazil has been of the countries most affected by the disease since the 1930 s. Approximately 99 % of cases are concentrated in the Amazon region, with the prevalence of infections by P*lasmodium vivax* and P*lasmodium falciparum* species representing a serious public health problem [3,4].

Plasmodium falciparum synthesizes Histidine-rich proteins (HRPs) during the asexual erythrocytic cycle. HRPs are biomolecules of approximately 30 kDa, soluble in water, and composed of amino acids histidine (73 %), alanine (7 %), proline (7.5 %), glutamic acid (6 %), and aspartic acid (2.1 %) [5]. Specifically, HRP2 is a stable molecule found in the parasite's cytoplasm and released abundantly into the host's bloodstream. Ag-*Pf*HRP2 can be detected in red blood cells, serum, plasma, cerebrospinal fluid, and urine of infected individuals, with a positive correlation between blood protein concentration and parasite biomass [6,7].

Currently, malaria tests are performed through microscopic methods (gold standard) or rapid diagnostic tests (RDTs). Also, other advanced techniques are used, such as Nucleic Acid Amplification Assays (NAATs) or Enzyme-Linked Immuno-Sorbent Assay (ELISA) [8–10]. During the last decades, various research groups have widely studied the development of biosensors for malaria biomarker determination [11–15]. Some authors have reported immunosensors for the detection of Ag-*Pf*HRP2, using its manufacture of diverse antibody immobilization methodologies on conductive substrates (gold or carbon electrodes) [16–21]. Generally, these antibodies (Ab-*Pf*HRP2) are produced in mice or rabbits, being G type immunoglobulins (IgG).

On the other hand, Immunoglobulins IgY constitutes an important fraction of egg yolk protein (equivalent to IgG in mammalian), which offers protection against pathogens to the embryo and chicks after birth. IgY is synthesized by plasma cells derived from B lymphocytes [22,23]. IgY possesses numerous advantages over mammalian IgG in high yield,

* Corresponding authors.
E-mail addresses: ariamna@ufam.edu.br (A. María Dip Gandarilla), wrbrito@ufam.edu.br (W. Ricardo Brito).

https://doi.org/10.1016/j.bioelechem.2022.108273
Received 11 August 2022; Received in revised form 12 September 2022; Accepted 16 September 2022
Available online 21 September 2022

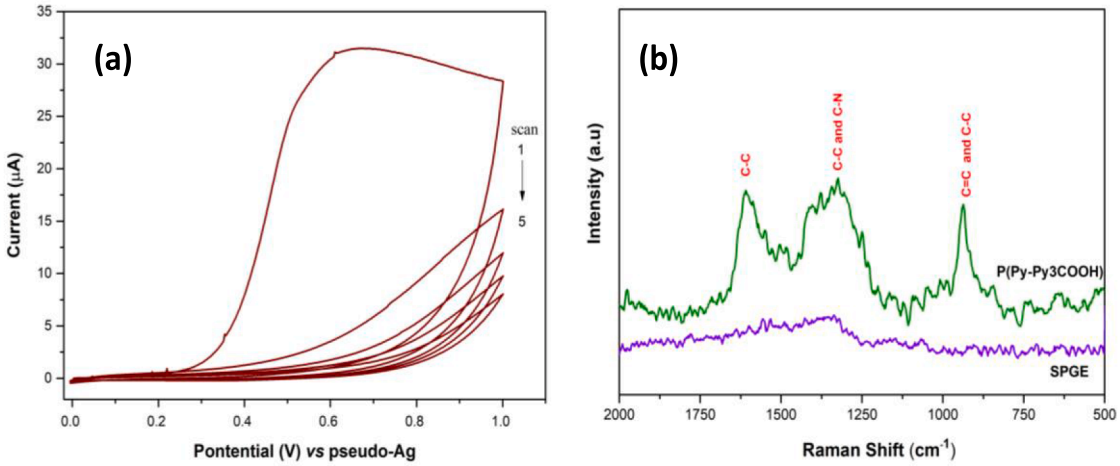

Fig. 1. (a) Voltammograms of the electropolymerization process of P(Py-Py3COOH) on SPGE surface, and (b) Raman spectra of bare SPGE and modified with P (Py-Py3COOH).

low cost, and convenience. In recent years the production of antibodies in avian (chicken) has attracted noticeable consideration, and numerous IgYs have been used against diverse antigens, for therapeutic purposes and for the development of immunoassays [24–27].

The antibodies immobilization onto electrodes modified with conducting polymers, such as carboxylated polypyrrole, is a strategy frequently used in the biosensor fabrication processes, where a covalent bond (amide type) is formed between antibodies and carboxylic groups present in the polymeric surface. The biosensor performance is studied by measuring their electrical properties through impedance or amperometric techniques [28–32]. PPy films and their derivatives can be obtained by applying an electrodeposition technique in an adequate monomeric solution [33–36].

In this work, we propose the use of Ab-*Pf*HRP2 (IgY) from egg yolk to develop a simple sensing platform based on screen-printed gold electrodes modified with P(Py-Py3CCOH) copolymer for the determination of Ag-*Pf*HRP2.

2. Materials and methods

2.1. Reagents

All reagents were of analytical grade, and the aqueous solutions were prepared using purified water from a Milli-Q system. Pyrrole, pyrrole 3-carboxylic acid, bovine serum albumin (BSA), N-(3-dimethylaminopropyl)-N'-ethylcarbodiimide hydrochloride (EDC), *N*-Hydroxysuccinimide (NHS), potassium hexacyanoferrate (III), carbonate-bicarbonate buffer of pH 9.60, tween 80 solution, glucose (Glu), glycine (Gly) and potassium chloride were purchased from Sigma-Aldrich (U.S.A). Potassium hexacyanoferrate (II) trihydrate, sulfuric acid (98 %), and phosphate buffer saline (PBS) of pH 7.00 were from Merck (Germany).

The biomolecules preparation process was performed in Leônidas and Maria Deane Institute (Oswaldo Cruz Foundation-Manaus/Brazil). Ag-*Pf*HRP2 consisted of a recombinant expression of *Plasmodium falciparum* HRP2 in *Escherichia coli* BL21 pLysS (Thermo Fisher Scientific, U.S.A), and the purification was performed using affinity chromatography nickel columns (Qiagen, Germany), following the manufacturer instructions [37]. 7-week-old Dekalb White laying hens were immunized with peptides coupled to solubilized carbon nanotubes. The antibodies (polyclonal Ab-*Pf*HRP2 (IgY type)) were extracted from chickens' yolks following the method described by Ko and Anh [38]. Peptide specific IgY antibodies were purified using a Sepharose resin coupled with the antigen. Besides, Ab-*Pf*HRP2 (IgG type) produced in mouse and Lactate dehydrogenase of *plasmodium vivax* (Ag-*Pv*LDH) were previously synthesized [21] and used in the ELISA test and selectivity studies, respectively.

2.2. Instrumentation

The chemical groups of the polymeric film were identified by Raman spectroscopy using a MacroRam spectrometer, Horiba Scientific (Japan), with a laser of 785 nm. Scanning electron microscopy (SEM) images were performed using a TESCAN microscope, VEGA3 model (France). First, the samples were placed on aluminum stubs with the aid of conductive carbon tape and covered with a thin gold layer in a Sputter Coater (Balzers SCD 050 model, Switzerland). Then, the samples were positioned in the microscope to 5 mm of the electron beam, and an intensity of 30 kV was applied. Elemental analysis of the surface was analyzed by Energy-dispersive X-ray spectroscopy (EDS), using an AZtec 4.3 EDS detector (Oxford Instruments, U.K), which is coupled to SEM.

The electrochemical data was collated in a PGSTAT128N potentiostat (Metrohm Autolab, Netherlands). SPGE (Metrohm Dropsens, Ref 220AT) was used as the conductive substrate, constituted by a gold working electrode (4 mm in diameter), gold auxiliary electrode, and pseudo-reference silver electrode. All the experiments were performed in triplicate and without stirring at room temperature (22 ± 1 °C).

2.3. Preparation of the immunosensor

First, the SPGEs were cleaned in 0.5 mol/L H_2SO_4 solution using cyclic voltammetry (CV) with potential between 0 and 1.2 V, at 100 mVs^{-1}, during 10 scans. Then, the electrodes were washed with Milli-Q water and dried with a nitrogen gas stream. A mixture of 0.05 mol/L pyrrole and 0.1 mol/L pyrrole-3 carboxylic acid prepared in 0.1 mol/L PBS pH 7.00 was employed as the monomeric solution. The copolymer was electrodeposited in the working electrode through 5 scans of CV, with a potential range of 0 to 1 V, at 20 mV s^{-1}. Afterward, the COOH groups present in the film surface were activated with 100 mmol/L EDC and 50 mmol/L NHS for 1 h. Following, 8 μL of IgY antibody (Ab-*Pf*HRP2) (0.2 μg μL^{-1}) was dripped in the working electrode and kept at 4 °C for 4 h in a humid chamber.

Blocking with 1 % BSA for 1 h was carried out to avoid non-specific binding between the antigen and the activated COOH groups. Finally, the immunosensor was incubated in Ag-*Pf*HRP2 solution (8 μL) at different concentrations (10–1000 ng mL^{1}) for 1 h. After each modification step, the SPGE was gently washed with Milli-Q water and dried at room temperature. The electrical response of the immunosensor was recorded during all modification steps in 5 mmol/L $K_3Fe(CN)_6/K_4Fe(CN)_6$ + 0.1 mol L^{-1} KCl solution, employing EIS at 0.1 V, varying the

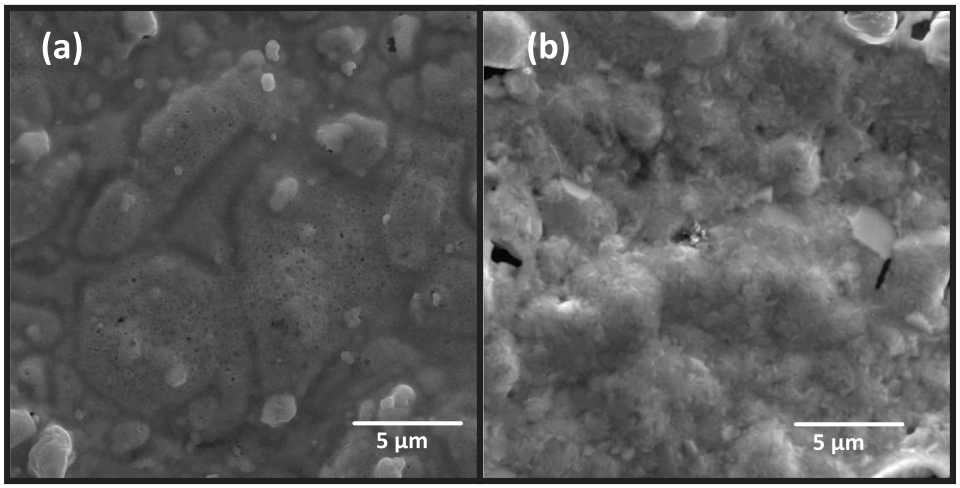

Fig. 2. SEM imagens at 16.7kx of (a) bare SPGE and (b) P(Py-Py3COOH)/SPGE.

frequency with logarithmic spacing frequency in the range from 1 kHz to 10 mHz, with amplitude of 0.01 V_{RMs}.

2.4. ELISA test

ELISA 96-well microtiter plates (SPL Life Sciences, South Korea) were sensitized for 2 h at 37 °C in a humid chamber, with 50 µL per well of a solution containing 4 µg mL^{-1} *Pf*HRP2 chicken antibodies diluted in 0.05 mol/L carbonate-bicarbonate buffer pH 9.60. After this period, the plates were washed with 10 mmol/L PBS containing 0.1 % tween 80 solution and then blocked for 2 h at 37 °C with 10 mmol/L PBS containing 0.1 % tween 80 solutions and 5 % BSA. Then, recombinant *Pf*HRP2 protein was added at different concentrations (100, 250, 500, 750, and 1000 $ngmL^{-1}$), and the resulting solutions were incubated for 16 h at 4 °C. Afterward, *Pf*HRP2 mouse antibodies were added at a concentration of 0.25 µg per well. These plates were incubated for 1 h at 37 °C in a humid chamber, followed by three washes with PBS containing 0.1 % tween 80 solution. Next, biotinylated goat anti-mouse IgG antibodies (Sigma Aldrich, U.S.A) were added at 1/5000 dilution and incubated again for 1 h at 37 °C in a humid chamber, the plate was washed as previously described. An additional incubation was performed by adding streptavidin conjugated with horseradish peroxidase (SeraCare KPL, U.S.A) at 1/5000 dilution and incubating for 1 h at 37 °C in a humid chamber. After a new cycle of three washes, 50 µL of one-step reagent (Scienco, Brazil) were added to the plate and incubated for 10 min at room temperature in the absence of light. The reaction was stopped with 25 µL of 1 mol/L H_2SO_4. The generated product was quantified by reading the optical density (O.D) at 450 nm in a spectrophotometer (LMR-96 model, Loccus, Brazil).

3. Results and discussion

The electropolymerization process using CV technique registered irreversible voltammograms (Fig. 1. a). During the first scan, there is an increase in the oxidation current values from 0.25 until 1 V, with a maximum oxidation peak at 0.6 V. In the subsequent scans, the oxidation currents gradually decrease, evidencing the growth of a brown film on the electrode surface, clearly visible to the human eye.

The chemical groups of the polymer were identified by Raman spectroscopy (Fig. 1. b). The spectra of the bare SPGE show a low intensity signal in 1441 cm^{-1}, which may be related to the presence of other organic compounds out coming from the gold ink [43]. The P(Py-Py3COOH) deposited on the electrode surface recorded three bands in the region of 500 to 2000 cm^{-1}, characteristic of the polypyrrole. The observed signal at 935 cm^{-1} is related to C—C ring deformation

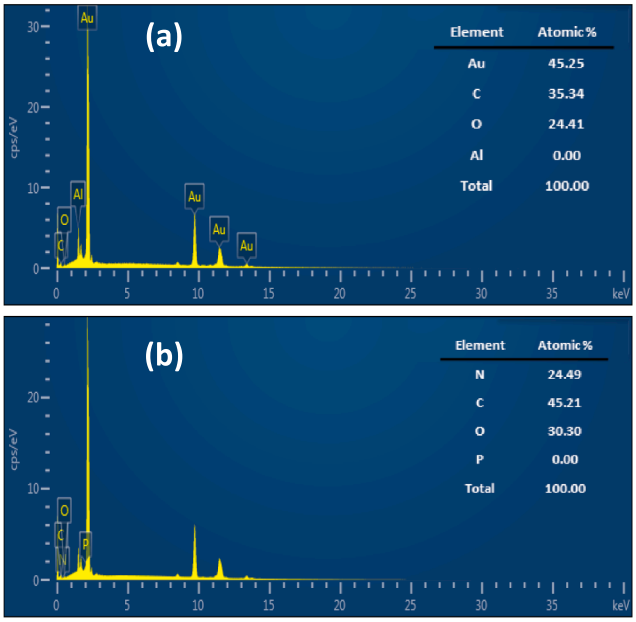

Fig. 3. EDS spectra of (a) bare SPGE surface and (b) SPGE surface modified with P(Py-Py3COOH).

(bipolarons). The D band recorded at 1330 cm^{-1} corresponds to C—C in the aromatic ring and antisymmetric C—N stretching. The G band at 1600 cm^{-1} is characteristic of C═C in-ring and C—C inter-ring stretching. Several authors have reported similar results for polypyrrole synthesized by chemical polymerization or electropolymerization techniques [39–42].

3.1. Morphological characterization

The morphological characterization of the SPGE modified with P(Py-Py3COOH) film was analyzed by SEM technique. The bare SPGE image (Fig. 2. a) reveals a heterogeneous and irregular surface, forming metal grains of different sizes. A porous surface (like a sponge) is observed, with ripples and holes. Other authors have reported similar characteristics for printed gold electrodes, and this fact may be associated with the deposition process of the gold ink during its manufacture [43,44].

After deposition of the polymeric film, the image evinces an increase in the irregularity of the surface, with scale-like structures, in a compact

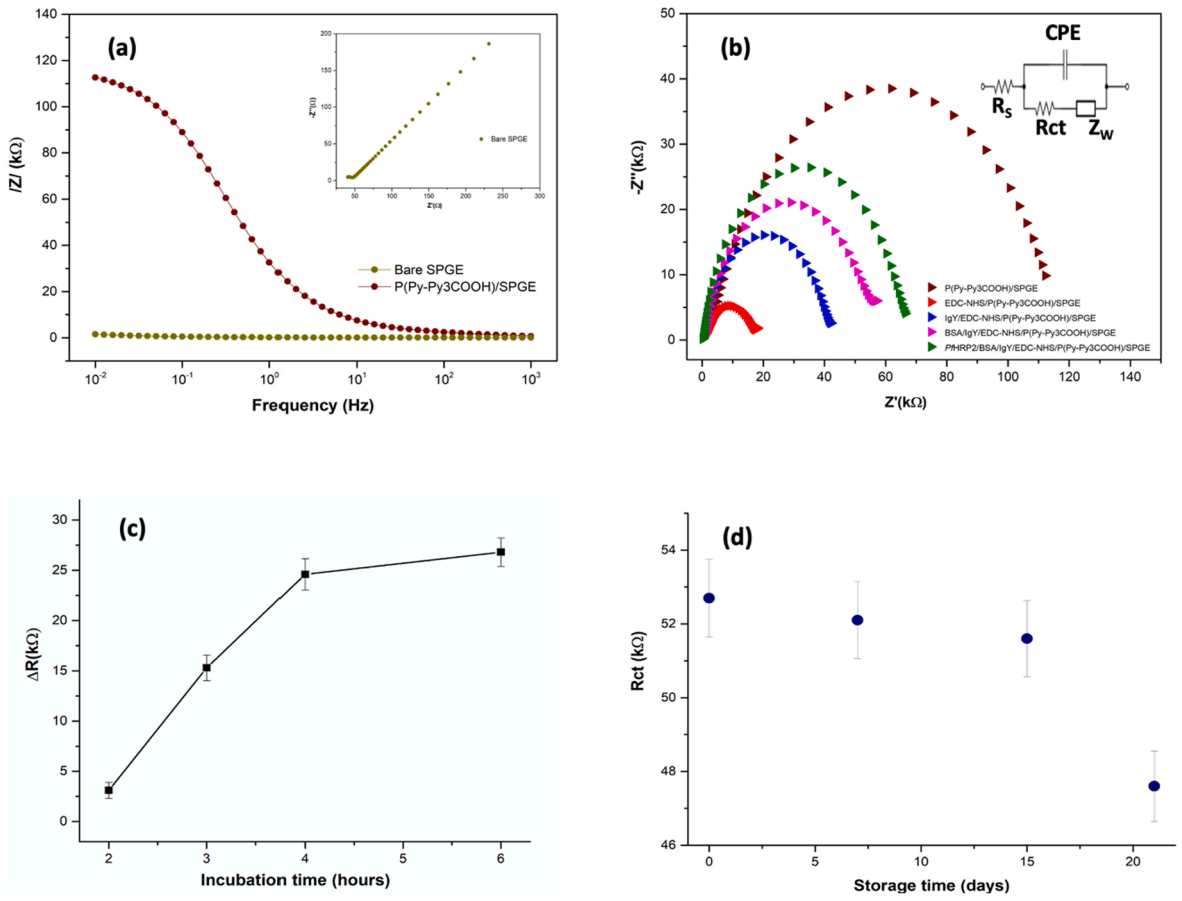

Fig. 4. (a) Bode graphic and (b) Nyquist graphic of the modification steps of SPGE recorded by EIS in $[Fe(CN)_6]^{4-/3-}$ + KCl solution. (c) Optimization of incubation time in antibody solution for IgY immobilization. (d) Impedimetric response of the immunosensor after storage for 3 weeks (mean values of Rct and standard deviation for three immunosensors).

form, which covers the surface of the gold electrode (Fig. 2. b).

Elemental analysis by EDS was performed to analyze the atomic composition of the polymeric surface. The EDS spectra of the bare gold SPGE (Fig. 3. a) revealed Au atoms (45 %) as the majority element. In addition, other elements, such as C and O, from the organic compounds used to manufacture the electrodes were detected, corroborating the results obtained by Raman spectroscopy [45].

On the other hand, the EDS spectra of the polymeric surface (Fig. 3. b) recorded nitrogen (24.94 %), carbon (45.21 %), and oxygen (30.30 %) atoms. These atoms make up the aromatic ring and functional groups of P(Py-Py3COOH), and their identification confirms the presence of the copolymer on the electrode surface.

3.2. Electrochemical characterization

The electrochemical characterization of *Pf*HRP2/BSA/IgY/P(Py-Py3COOH)/SPGE fabrication steps were followed by EIS (Fig. 4) and the Rct values calculated by iterative fitting (NOVA 2.1.5 software) of the experimental data to the Randles equivalent circuit (Fig. 4. b, inset). Here, the resistance of the solution, contacts, and connections (Rs), and charge transference resistance (Rct) are measured at the high frequency region. The linear part at lower frequencies is the impedance described by Warburg (Zw) and is related to the mass transfer of the redox species to the electrode (diffusion process). The constant phase element (CPE) is the impedance of the electrode/solution interface. The Z_W and Rs are not affected significantly by the modifications that occur on the electrode surface. Therefore, the capacitance and Rct parameters are mainly used in impedimetric sensors [46]. In this work, the Rct values were used to determine the electrodes interfacial properties using redox couples ($[Fe(CN)_6]^{4-/3-}$) in the solution.

The impedimetric response of bare SPGE showed a profile non-resistive, with a small semicircle at high frequencies and low values of Rct = 7.71 Ω (Nyquist diagram, Fig. 4. a, inset). After electropolymerization of P(Py-Py3COOH) on SPGE, the electrode recorded a highly resistive profile, and the impedance values (|Z|) evidenced remarkable increases when compared to the bare electrode (Bode diagram, Fig. 4. a). In the Nyquist diagram (Fig. 4. b), the polymeric film (P(Py-Py3COOH)/SPGE) exhibited a large semicircle with high Rct values (115 kΩ). This behavior is due to the insulating characteristics of the copolymer, which are intensified by the presence on the surface of COOH groups, negatively charged, that interact repulsively with the electrochemical probe ($[Fe(CN)_6]^{4-/3-}$), with negative charges too [32,46].

In the next step, the COOH groups were activated with EDC/NHS coupling agents and was observed a notable decrease in the resistance values (15.9 kΩ) (Fig. 4. b). This behavior can be attributed to the attraction between the NH_2 groups (positively charged) of intermediate esters formed in the activation process and the electrochemical probe (negatively charged). The reactions using EDC/NHS are widely used for covalent coupling of biomolecules to surfaces modified. Several authors have reported these methodologies in immunosensor manufacture, resulting in devices with excellent performance for antigen detection [32,47,48]. After IgY immobilization and block with BSA were registered (for both modifications), an increase of the semicircle curve and Rct values of 40.5 kΩ and 53.0 kΩ, respectively. Here, the electrode surface is partially blocked by the presence of structures with large molecular sizes that limit the charge transference [21]. Finally, an even higher hindrance effect (Rct = 65.3 kΩ) was noticed when the

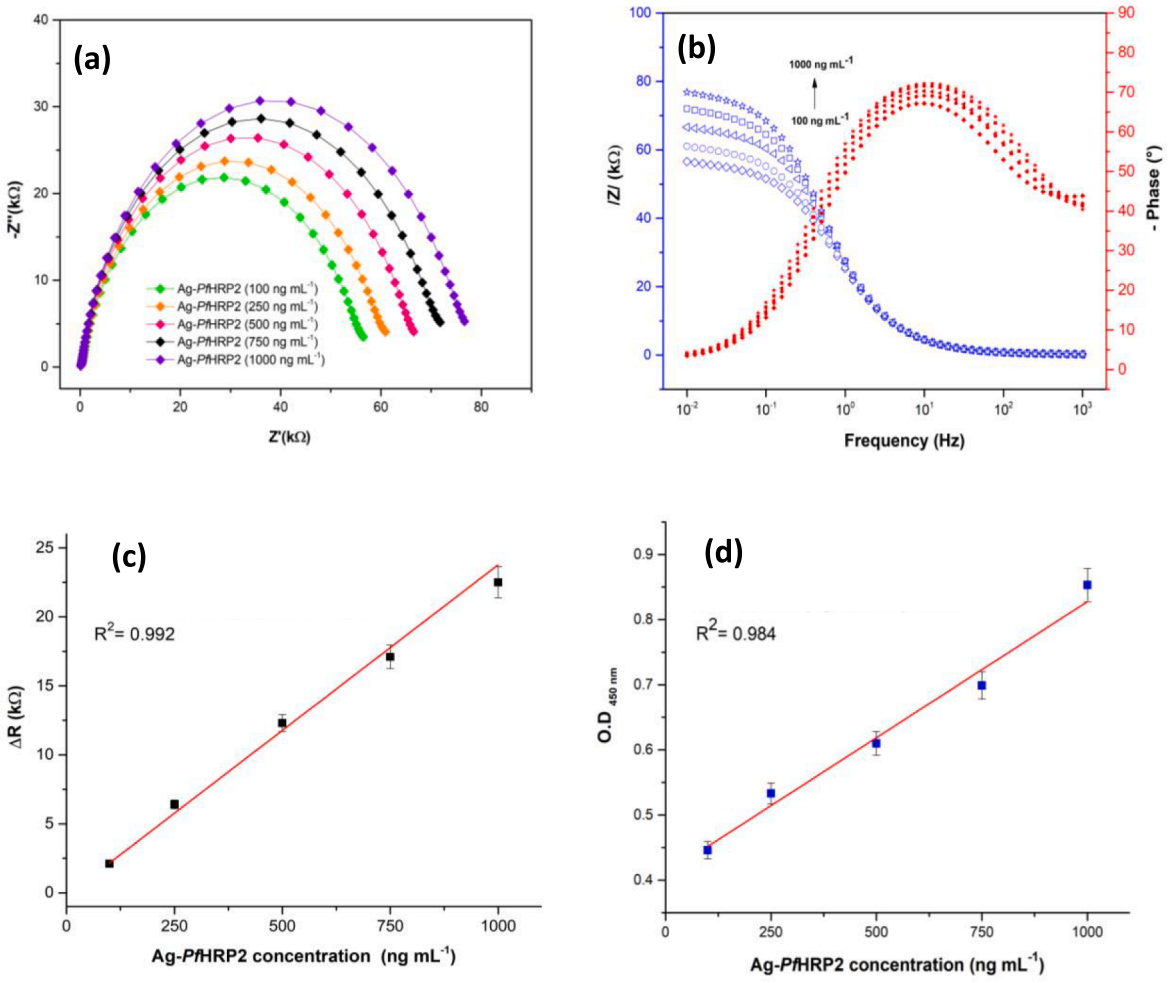

Fig. 5. EIS spectra (a) Nyquist graphic and (b) Bode graphic recorded in $[Fe(CN)_6]^{4-/3-}$+ KCl solution using the immunosensor upon addition of Ag-*Pf*HRP2 at different concentrations. (c) Calibration curve (ΔR vs Ag-*Pf*HRP2 concentration, equation curve: ΔR(kΩ) = 0.024[*Ag-PfHRP2*]-0.237 with R^2 = 0.992) and (d) Calibration curve obtained by ELISA test (O.D vs Ag-*Pf*HRP2 concentration, equation curve: O.D = 4.17x10^{-4}[Ag-*Pf*HRP2] + 0.409 with R^2 = 0.984).

immunosensor was incubated in Ag-*Pf*HRP2 solution (500 ng mL^{-1}), caused by the formation of the antibody-antigen complex.

The optimization of Ab-*Pf*HRP2 (IgY) incubation time is an important step that allows us to reduce fabrication times and obtain an immunosensor with better performance during the detection of the target analyte. Various incubation times were studied (2, 3, 4, and 6 h), and the electrochemical response was measured by EIS. The variation of charge transference (ΔR) was calculated, where ΔR = Rct $_{(after\ IgY)}$ - Rct $_{(before\ IgY)}$. The results of Fig. 4. c exhibit an increase of ΔR values with the incubation time until 4 h. Non-considerable ΔR increases were noticed at higher incubation time hence 4 h was adopted as the optimum time for the Ab-*Pf*HRP2 (IgY) immobilization.

Another parameter, such as Ab-*Pf*HRP2 (IgY) concentration, was used according to Figuereido *et al.* They utilized antibodies from egg yolk (IgY type) of 0.2 μg μL^{-1} concentration for the development of an immunosensor for dengue detection, and under these experimental conditions, the device showed good performance [49].

Reproducibility studies were performed to evaluate the stability of the immunosensor. Three BSA/Ab-*Pf*HRP2(IgY)/P(Py-Py3COOH)/SPGE immunosensors were manufactured and stored in a moist chamber at 4 °C for 3 weeks. The impedimetric response of each immunosensor was collected for 7, 15, and 21 days. The results showed reproducibility and good stability up to 15 days of storage (Fig. 4. d) without remarkable variation in the Rct values. After 21 days, the Rct decreased ~ 10 %.

3.3. Determination of Ag-PfHRP2

The analytical performance of the immunosensor was examined with Ag-*Pf*HRP2 standard solutions (n = 6) at different concentrations: 10, 100, 250, 500, 750, and 1000 ng mL^{-1} prepared in 0.1 mol/L PBS pH 7.00. The EIS spectra of Fig. 5. a (Nyquist diagram) shows an increase of the semicircle curve with the increase of antigen concentration and higher values of |Z|, and phase angle is recorded when concentration increases until 1000 ng mL^{-1} (Bode diagram, Fig. 5. b). The calibration curve was obtained by plotting ΔR(kΩ) (ΔR = Rct$_{(after\ Ag\text{-}PfHRP2)}$ - Rct$_{(before\ Ag\text{-}PfHRP2)}$) *versus* *Pf*HRP2 concentration (Fig. 5. c). The linear relationship was established from 100 to 1000 ng mL^{-1} Ag-*Pf*HRP2, and the LOD calculated was 27.47 ng mL^{-1}. The curve equation was defined as ΔR(kΩ) = 0.024[*Ag-PfHRP2*]-0.237, with R^2 = 0.992. According to the reports of other authors [50,51], this concentration range can be associated with severe malaria.

Also, experiments through the ELISA technique were performed to confirm the results obtained by EIS for Ag-P*f*HRP2 determination. The calibration curve was obtained by plotting optical density (O.D.) vs Ag-*Pf*HRP2 concentration (Fig. 5. d). The results show a linear relationship in the concentration range from 100 − 1000 ng mL^{-1}, with a LOD of 53.95 ng mL^{-1}. The curve equation was defined as O.D = 4.17x10^{-4}[Ag-*Pf*HRP2] + 0.409, with R^2 = 0.984.

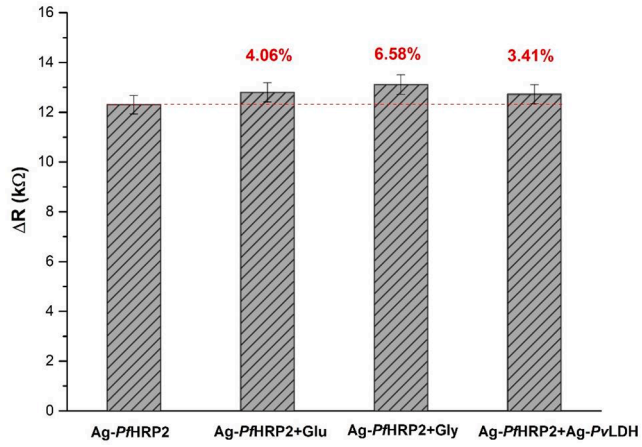

Fig. 6. Electrochemical response of immunosensor after incubation in binary solutions (Ag-*Pf*HRP2 + interfering) recorded by EIS in $Fe(CN)_6]^{4-/3-}$+ KCl solution.

Table 1
Comparison with other methods reported for Ag-*Pf*HRP2 detection.

System	Method Principle	LOD	Reference
Immunoassay	Malaria ELISA kit	25 pg mL^{-1}	[55]
Immunoassay	Antibodies (IgG) conjugated to magnetic spheres and quantum dots.	0.5 ng mL^{-1}	[51]
Immunosensor	Gold electrodes modified with colloidal gold nanoparticles and antibodies (IgG).	36 pg mL^{-1}	[56]
Immunosensor	Graphite-epoxy electrodes modified with antibodies (IgG) linked to magnetic beads and nanoparticles.	0.36 ng mL^{-1}	[57]
Immunosensor	Gold electrodes modified with carbon nanotubes-ZnO nanofibers and antibodies (IgG).	0.97 fg mL^{-1}	[58]
Immunosensor	Gold coated quartz crystal modified with self-assembled monolayers of thioctic acid, 1-dodecanethiol and antibodies (IgG).	12 ng mL^{-1}	[17]
Aptasensor	Gold electrodes modified with di-thiobis-succinimidyl propionate and amine-functionalized aptamer.	3.15 pmol/L	[19]
Immunosensor	Indium tin oxide electrodes modified with primary antibody (IgG) and methylene blue labeled secondary antibody	1 pg mL^{-1}	[59]
Immunosensor	Gold disc electrodes modified with a polymeric matrix of dihexadecyl phosphate and antibodies (IgG).	3.3 ng mL^{-1}	[21]
Immunosensor	SPGE modified with carboxylated polypyrrole films and antibodies (IgY).	27.47 ng mL^{-1}	This work

3.4. Selectivity study of the immunosensor

The selectivity tests constitute an important step in the development of immunosensors because they allow the evaluation of the possibility of application in real samples without interference from other molecules. The immunosensor was incubated for 1 h in binary solutions (Ag-*Pf*HRP2 + Glucose, Ag-*Pf*HRP2 + Glycine, and Ag-*Pf*HRP2 + Ag-*Pv*LDH), each component at 500 ng mL^{-1}. Later the impedimetric response was measured by EIS under the same experimental conditions used in Ag-*Pf*HRP2 determination. The ΔR was calculated from the Rct values (obtained from Nyquist diagram) before and after incubation in each binary solution. The results of Fig. 6 indicate a low rebinding for glucose (4.06 %), glycine (6.58 %), and Ag-*Pv*LDH (3.41 %), suggesting that the immunosensor presents good selectivity for Ag-*Pf*HRP2 determination. Other works with values until 11 % have considered the biosensors with an affinity for the target molecule [52–54].

Table 1 shows other methods reported for the determination of Ag-*Pf*HRP2. The immunosensor described in this work showed stability and good performance, and the registered LOD is acceptable compared to the methodologies reported in Table 1. Our method uses egg yolk antibodies and has not been applied in developing immunosensors for Ag-*Pf*HRP2 detection. The proposed immunosensor is simple, based on antibodies immobilization on polypyrrole thin films through covalent binding, label-free and direct detection of antigens. However, it uses cheaper materials than the reported methods, which use complicated methodologies, and expensive reagents such as carbon nanotubes, nanoparticles, magnetic spheres, ionic liquids, nanofibers, or quantum dots.

4. Conclusions

In summary, we explore the application of (IgY) egg yolk antibodies to develop an impedimetric immunosensor for the determination of *Pf*HRP2 antigen. The electropolymerization of a polymeric film on SPGE was performed successfully, and Ab-*Pf*HRP2 (IgY) was immobilized (through covalent bonding) on P(Py-Py3COOH)/SPGE surface. The immunosensor showed excellent performance in the concentration range of 100 to 1000 ng mL^{-1}, with LOD of 27.47 ng mL^{-1}. The device could detect other molecules less than 7 % for all the compounds tested. The immunosensor presents simplicity, short manufacture time, stability and high sensitivity, and selectivity using IgY type antibodies, which constitute attractive advantages for application in human serum samples from a patient with malaria caused by *Plasmodium falciparum*.

Declaration of Competing Interest

The authors declare that they have no known competing financial interests or personal relationships that could have appeared to influence the work reported in this paper.

Data availability

Data will be made available on request.

Acknowledgments

The authors would like to thank for the financial support to Coordenação de Aperfeiçoamento de Pessoal de Nível Superior (CAPES), Universidade Federal do Amazonas (UFAM), Fundação de Amparo à Pesquisa do Estado do Amazonas (FAPEAM) and Bio-manguinhos-FIOCRUZ.

References

[1] World Health Organization, World Malaria Report: 20 years of global progress and challenges, (2020). https://www.who.int/publications/i/item/9789240015791. Accessed 26 June 2022.
[2] A.M. Gimenez, R.F. Marques, M. Regiart, D.Y. Bargieri, Diagnostic Methods for Non-Falciparum Malaria, Front. Cell. Infect. Microbiol. 11 (2021) 1–24, https://doi.org/10.3389/fcimb.2021.681063.
[3] Ministério da Saúde/ Secretaria de Vigilância em Saúde, Boletim Epidemiológico. Malária-2020, (2020). https://www.gov.br/saude/pt-br/assuntos/media/pdf/2020/dezembro/03/boletim_especial_malaria_1dez20_final.pdf. Accessed 29 May 2022.
[4] L. Deane, Os grandes marcos na história do controle da malária, Rev Soc Bras Med Trop. 25 (1992) 12–22.
[5] E.L. Schneider, M.A. Marletta, Heme binding to the histidine-rich protein II from *Plasmodium falciparum*, Biochemistry. 44 (2005) 979–986, https://doi.org/10.1021/bi048570p.
[6] P. Jain, B. Chakma, S. Patra, P. Goswami, Potential biomarkers and their applications for rapid and reliable detection of malaria, Biomed Res. Int. 2014 (2014) 1–20, https://doi.org/10.1155/2014/852645.
[7] J.C. Mouatcho, J.P. Dean Goldring, Malaria rapid diagnostic tests: Challenges and prospects, J. Med. Microbiol. 62 (2013) 1491–1505, https://doi.org/10.1099/jmm.0.052506-0.
[8] A. Moody, Rapid diagnostic tests for malaria, Clin. Microbiol. Rev. 15 (2002) 66–78, https://doi.org/10.1128/CMR.15.1.66-78.2002.

[9] J.H. Kattenberg, E.A. Ochodo, K.R. Boer, H.D. Schallig, P.F. Mens, M.M. Leeflang, Systematic review and meta-analysis: Rapid diagnostic tests versus placental histology, microscopy and PCR for malaria in pregnant women, Malar. J. 10 (2011) 1–18, https://doi.org/10.1186/1475-2875-10-321.

[10] K. Abba, J. Deeks, P. Olliaro, C. Naing, S. Jackson, Y. Takwoingi, S. Donegan, P. Garner, Rapid diagnostic tests for diagnosing uncomplicated *P. falciparum* malaria in endemic countries (Review), Cochrane Database Syst. Rev., CD008122 (2012), 10.1002/14651858.CD008122.pub2.

[11] K. Ragavan, S. Kumar, S. Swaraj, S. Neethirajan, Advances in biosensors and optical assays for diagnosis and detection of malaria, Biosens. Bioelectron. 105 (2018) 188–210, https://doi.org/10.1016/j.bios.2018.01.037.

[12] D.X. Liu, T.T.T. Tien, D.T. Bao, N.T.P. Linh, H. Park, S.J. Yeo, A novel peptide aptamer to detect *plasmodium falciparum* lactate dehydrogenase, J. Biomed. Nanotechnol. 15 (2019) 204–211, https://doi.org/10.1166/jbn.2019.2667.

[13] Y.K. Low, J. Chan, G.V. Soraya, C. Bu, C.D. Abeyrathne, D.H. Huynh, E. Skafidas, P. Kwan, Development of an Ultrasensitive Impedimetric Immunosensor Platform for Detection of *Plasmodium* Lactate Dehydrogenase, Sensors. 19 (2019) 2446, https://doi.org/10.3390/s19112446.

[14] A. Hemben, J. Ashley, I.E. Tothill, An immunosensor for parasite lactate dehydrogenase detection as a malaria biomarker – Comparison with commercial test kit, Talanta. 187 (2018) 321–329, https://doi.org/10.1016/j.talanta.2018.04.086.

[15] M. Regiart, A.M. Gimenez, R.F. Marques, I.S. Soares, M. Bertotti, Microfluidic device based on electrodeposited Nanoporous Gold/Carbon Nanotubes for *Plasmodium vivax* detection, Sensors Actuators B Chem. 340 (2021), 129961, https://doi.org/10.1016/j.snb.2021.129961.

[16] M.K. Sharma, V.K. Rao, G.S. Agarwal, G.P. Rai, N. Gopalan, S. Prakash, S. K. Sharma, R. Vijayaraghavan, Highly sensitive amperometric immunosensor for detection of plasmodium falciparum histidine-rich protein 2 in serum of humans with malaria: Comparison with a commercial kit, J. Clin. Microbiol. 46 (2008) 3759–3765, https://doi.org/10.1128/JCM.01022-08.

[17] M.K. Sharma, V.K. Rao, S. Merwyn, G.S. Agarwal, S. Upadhyay, R. Vijayaraghavan, A novel piezoelectric immunosensor for the detection of malarial *Plasmodium falciparum* histidine rich protein-2 antigen, Talanta. 85 (2011) 1812–1817, https://doi.org/10.1016/j.talanta.2011.07.008.

[18] A. Hemben, J. Ashley, Development of an Immunosensor for *Pf*HRP2 as a Biomarker for Malaria Detection, Biosensors. 7 (2017) 28, https://doi.org/10.3390/bios7030028.

[19] B. Chakma, P. Jain, N.K. Singh, P. Goswami, Development of Electrochemical Impedance Spectroscopy Based Malaria Aptasensor Using HRP-II as Target Biomarker, Electroanalysis. 30 (2018) 1839–1846, https://doi.org/10.1002/elan.201800142.

[20] K.B. Paul, S. Kumar, S. Tripathy, S.R.K. Vanjari, V. Singh, S. Singh, A highly sensitive self assembled monolayer modified copper doped zinc oxide nanofiber interface for detection of *Plasmodium falciparum* histidine-rich protein-2: Targeted towards rapid, early diagnosis of malaria, Biosens. Bioelectron. 80 (2016) 39–46, https://doi.org/10.1016/j.bios.2016.01.036.

[21] A.M.D. Gandarilla, M. Regiart, M. Bertotti, J.C. Glória, L.A.M. Mariuba, W.R. Brito, One-step enzyme-free dual electrochemical immunosensor for histidine-rich protein 2 determination, RSC Adv. 11 (2021) 408–415, https://doi.org/10.1039/d0ra08729g.

[22] S. Réhault-Godbert, N. Guyot, Vitellogenesis and yolk proteins, birds, In: M. Skinner (Ed.), Encycl. Reprod., 2018, pp. 278–284, 10.1016/B978-0-12-809633-8.20568-2.

[23] N.M. Lanzarini, G.A. Bentes, E. de M. Volotão, M.A. Pinto, Use of chicken immunoglobulin Y in general virology, J. Immunoass. Immunochem., 39 (2018), pp. 235–248, 10.1080/15321819.2018.1500375.

[24] G. Brunda, R.B. Sashidhar, R.K. Sarin, Use of egg yolk antibody (IgY) as an immunoanalytical tool in the detection of Indian cobra (Naja naja naja) venom in biological samples of forensic origin, Toxicon. 48 (2006) 183–194, https://doi.org/10.1016/j.toxicon.2006.04.011.

[25] D. Thirumalai, S. Visaga Ambi, R.S. Vieira-Pires, Z. Xiaoying, S. Sekaran, U. Krishnan, Chicken egg yolk antibody (IgY) as diagnostics and therapeutics in parasitic infections – A review, Int. J. Biol. Macromol. 136 (2019) 755–763, https://doi.org/10.1016/j.ijbiomac.2019.06.118.

[26] R.G.E. Krause, A.F. Grobler, J.P.D. Goldring, Comparing Antibody Responses in Chickens Against *Plasmodium falciparum* Lactate Dehydrogenase and Glyceraldehyde-3-phosphate Dehydrogenase with Freunds and Pheroid® Adjuvants, Immunol. Invest. 44 (2015) 627–642, https://doi.org/10.3109/08820139.2015.1070268.

[27] S. Gandhi, N. Caplash, P. Sharma, C. Raman Suri, Strip-based immunochromatographic assay using specific egg yolk antibodies for rapid detection of morphine in urine samples, Biosens. Bioelectron. 25 (2009) 502–505, https://doi.org/10.1016/j.bios.2009.07.018.

[28] H. Zejli, K.Y. Goud, J.L. Marty, Label free aptasensor for ochratoxin A detection using polythiophene-3-carboxylic acid, Talanta. 185 (2018) 513–519, https://doi.org/10.1016/j.talanta.2018.03.089.

[29] W. Thunyakontirakun, S. Sriwichai, S. Phanichphant, R. Janmanee, Fabrication of poly(pyrrole-3-carboxylic acid)/graphene oxide composite thin film for glucose biosensor, Mater. Today Proc. 17 (2019) 2070–2077, https://doi.org/10.1016/j.matpr.2019.06.255.

[30] R. Janmanee, A. Baba, S. Phanichphant, S. Sriwichai, K. Shinbo, K. Kato, F. Kaneko, Detection of human IgG on Poly(pyrrole-3-carboxylic acid) thin film by electrochemical-Surface plasmon resonance spectroscopy, Jpn. J. Appl. Phys. 50 (2011) 01BK02, https://doi.org/10.1143/JJAP.50.01BK02.

[31] R. Khoder, H. Korri-Youssoufi, E-DNA biosensors of *M. tuberculosis* based on nanostructured polypyrrole, Mater. Sci. Eng. C. 108 (2020), 110371, https://doi.org/10.1016/j.msec.2019.110371.

[32] G. Yuan, J. He, Y. Li, W. Xu, L. Gao, C. Yu, A novel ultrasensitive electrochemical immunosensor based on carboxy-endcapped conductive polypyrrole for the detection of gypican-3 in human serum, Anal. Methods. 7 (2015) 1745–1750, https://doi.org/10.1039/c4ay02820a.

[33] J. Husson, S. Lakard, S. Monney, C.C. Buron, B. Lakard, Elaboration and characterization of carboxylic acid-functionalized polypyrrole films, Synth. Met. 220 (2016) 247–254, https://doi.org/10.1016/j.synthmet.2016.06.017.

[34] A.M.R. Ramírez, M.A. Gacitúa, E. Ortega, F.R. Díaz, M.A. del Valle, Electrochemical *in situ* synthesis of polypyrrole nanowires, Electrochem. Commun. 102 (2019) 94–98, https://doi.org/10.1016/j.elecom.2019.04.007.

[35] C. Debiemme-Chouvy, A. Fakhry, F. Pillier, Electrosynthesis of polypyrrole nano/micro structures using an electrogenerated oriented polypyrrole nanowire array as framework, Electrochim. Acta. 268 (2018) 66–72, https://doi.org/10.1016/j.electacta.2018.02.092.

[36] J.A. Luceño-Sánchez, A.M. Díez-Pascual, Grafting of polypyrrole-3-carboxylic acid to the surface of hexamethylene diisocyanate-functionalized graphene oxide, Nanomaterials. 9 (2019) 1–20, https://doi.org/10.3390/nano9081095.

[37] L.P. Sousa, L.A.M. Mariuba, R.J. Holanda, J.P. Pimentel, M.E.M. Almeida, Y. O. Chaves, D. Borges, E. Lima, J.L. Crainey, P.P. Orlandi, M.V. Lacerda, P. A. Nogueira, A novel polyclonal antibody-based sandwich ELISA for detection of *Plasmodium vivax* developed from two lactate dehydrogenase protein segments, BMC Infect. Dis. 14 (2014) 1–8, https://doi.org/10.1186/1471-2334-14-49.

[38] K.Y. Ko, D.U. Ahn, Preparation of Immunoglobulin Y from Egg Yolk Using Ammonium Sulfate Precipitation and Ion Exchange Chromatography, Poult. Sci., 86 (2007), pp. 400–407, 10.1093A/ps/86.2.400.

[39] M. Šetka, R. Calavia, L. Vojkůvka, E. Llobet, J. Drbohlavová, S. Vallejos, Raman and XPS studies of ammonia sensitive polypyrrole nanorods and nanoparticles, Sci. Rep. 9 (2019) 1–10, https://doi.org/10.1038/s41598-019-44900-1.

[40] X. Tang, T. Liu, H. Li, D. Yang, L. Chen, X. Tang, Notably enhanced thermoelectric properties of lamellar polypyrrole by doping with β-naphthalene sulfonic acid, RSC Adv. 7 (2017) 20192–20200, https://doi.org/10.1039/c7ra02302b.

[41] S. Kim, L.K. Jang, H.S. Park, J.Y. Lee, Electrochemical deposition of conductive and adhesive polypyrrole-dopamine films, Sci. Rep. 6 (2016) 1–8, pp. 10.1038/srep30475.

[42] Y.M. Choi, H. Lim, H.N. Lee, Y.M. Park, J.S. Park, H.J. Kim, Selective Nonenzymatic Amperometric Detection of Lactic Acid in Human Sweat Utilizing a Multi-Walled Carbon Nanotube (MWCNT)-Polypyrrole Core-Shell Nanowire, Biosensors. 10 (2020) 1–10, https://doi.org/10.3390/bios10090111.

[43] B. Saha, P. Songe, T.H. Evers, M.W.J. Prins, The influence of covalent immobilization conditions on antibody accessibility on nanoparticles, Analyst. 142 (2017) 4247–4256, https://doi.org/10.1039/c7an01424d.

[44] E. Verheyen, J.P. Schillemans, M. Van Wijk, M. Demeniex, W.E. Hennink, C.F. Van Nostrum, Challenges for the effective molecular imprinting of proteins, Biomaterials. 32 (2011) 3008–3020, https://doi.org/10.1016/j.biomaterials.2011.01.007.

[45] R.S. Gomes, F.T.C. Moreira, R. Fernandes, M.F. Goreti Sales, Sensing CA 15–3 in point-of-care by electropolymerizing O-phenylenediamine (oPDA) on Au-screen printed electrodes, PLoS One. 13 (2018) 1–19, https://doi.org/10.1371/journal.pone.0196656.

[46] L.T.N. Truong, M. Chikae, Y. Ukita, Y. Takamura, Labelless impedance immunosensor based on polypyrrole – pyrolecarboxylic acid copolymer for hCG detection, Talanta. 85 (2011) 2576–2580, https://doi.org/10.1016/j.talanta.2011.08.018.

[47] M. Tertis, A. Cernat, M. Suciu, R. Sa, C. Cristea, Poly- (pyrrole-3-carboxylic acid) Based Nanostructured Platform for the Detection of Carcinoembryonic Antigen, Electroanalysis. 30 (2018) 1100–1106, https://doi.org/10.1002/elan.201700803.

[48] R. Singh, S. Hong, J. Jang, Label-free Detection of Influenza Viruses using a Reduced Graphene Oxide-based Electrochemical Immunosensor Integrated with a Microfluidic Platform, Sci. Rep. 7 (2017) 1–11, https://doi.org/10.1038/srep42771.

[49] A. Figueiredo, N.C.S. Vieira, J.F. Dos Santos, B.C. Janegitz, S.M. Aoki, P.P. Junior, R.L. Lovato, M.L. Nogueira, V. Zucolotto, F.E.G. Guimarães, Electrical detection of dengue biomarker using egg yolk immunoglobulin as the biological recognition element, Sci. Rep. 5 (2015) 1–5, https://doi.org/10.1038/srep07865.

[50] I.C.E. Hendriksen, L.J. White, J. Veenemans, G. Mtove, C. Woodrow, B. Amos, S. Saiwaew, S. Gesase, B. Nadjm, K. Silamut, S. Joseph, K. Chotivanich, N.P.J. Day, L. Von Seidlein, H. Verhoef, H. Reyburn, N.J. White, A.M. Dondorp, Defining *falciparum*-malaria-attributable severe febrile illness in moderate-to-high transmission settings on the basis of plasma *Pf*HRP2 concentration, J. Infect. Dis. 207 (2013) 351–361, https://doi.org/10.1093/infdis/jis675.

[51] Y.E. Castro-Sesquen, C. Kim, R.H. Gilman, D.J. Sullivan, P.C. Searson, Nanoparticle-Based Histidine-Rich Protein-2 Assay for the Detection of the Malaria Parasite *Plasmodium falciparum*, Am. J. Trop. Med. Hyg. 95 (2016) 354–357, https://doi.org/10.4269/ajtmh.15-0772.

[52] A.M.D. Gandarilla, R.S. Matos, Y.R. Barcelay, H.D. Fonseca Filho, W.R. Brito, Molecularly imprinted polymer on indium tin oxide substrate for bovine serum albumin determination, J. Polym. Res., 29, 166 (2022), pp. 1–11, 10.1007/s10965-022-03022-5.

[53] A.P.M. Tavares, M.G.F. Sales, Novel electro-polymerized protein-imprinted materials using Eriochrome black T: Application to BSA sensing, Electrochim. Acta. 262 (2018) 214–225, https://doi.org/10.1016/j.electacta.2017.12.191.

[54] A.M.D. Gandarilla, J.C. Glória, Y.R. Barcelay, L.A.M. Mariuba, W.R. Brito, Electrochemical immunosensor for detection of *Plasmodium vivax* lactate

dehydrogenase, Mem. Inst. Oswaldo Cruz. 117 (2022) 1–6, https://doi.org/10.1590/0074-02760220085.
[55] I.K. Jang, S. Das, R.S. Barney, R.B. Peck, A. Rashid, S. Proux, E. Arinaitwe, J. Rek, M. Murphy, K. Bowers, S. Boadi, J. Watson, F. Nosten, B. Greenhouse, P. L. Chiodini, G.J. Domingo, A new highly sensitive enzyme-linked immunosorbent assay for the detection of *Plasmodium falciparum* histidine-rich protein 2 in whole blood, Malar. J. 17 (2018) 1–8, https://doi.org/10.1186/s12936-018-2545-5.
[56] A. Hemben, J. Ashley, I.E. Tothill, Development of an Immunosensor for *Pf*HRP2 as a biomarker for malaria detection, Biosensors. 7 (2017) 1–14, https://doi.org/10.3390/bios7030028.
[57] M. De Souza Castilho, T. Laube, H. Yamanaka, S. Alegret, M.I. Pividori, Magneto immunoassays for *plasmodium falciparum* histidine-rich protein 2 related to malaria based on magnetic nanoparticles, Anal. Chem. 83 (2011) 5570–5577, https://doi.org/10.1021/ac200573s.
[58] K. Paul, A.K. Panigrahi, V. Singh, S.G. Singh, A multi-walled carbon nanotube-zinc oxide nanofiber based flexible chemiresistive biosensor for malaria biomarker detection, Analyst. 142 (2017) 2128–2135, https://doi.org/10.1039/c7an00243b.
[59] G. Dutta, S. Nagarajan, L.J. Lapidus, P.B. Lillehoj, Enzyme-free electrochemical immunosensor based on methylene blue and the electro-oxidation of hydrazine on Pt nanoparticles, Biosens. Bioelectron. 92 (2017) 372–377, https://doi.org/10.1016/j.bios.2016.10.094.